

Rapid formation of H_3^+ from ammonia and methane following 4 MeV proton impact

This article has been downloaded from IOPscience. Please scroll down to see the full text article.

2009 J. Phys. B: At. Mol. Opt. Phys. 42 091002

(<http://iopscience.iop.org/0953-4075/42/9/091002>)

View [the table of contents for this issue](#), or go to the [journal homepage](#) for more

Download details:

IP Address: 38.107.179.212

The article was downloaded on 21/02/2012 at 14:32

Please note that [terms and conditions apply](#).

FAST TRACK COMMUNICATION

Rapid formation of H_3^+ from ammonia and methane following 4 MeV proton impact

Bethany Jochim¹, Amy Lueking^{1,3}, Laura Doshier^{1,3}, Sharayah Carey¹,
E Wells¹, Eli Parke^{2,4}, M Leonard^{2,5}, K D Carnes² and I Ben-Itzhak²

¹ Department of Physics, Augustana College, Sioux Falls, SD 57197, USA

² James R Macdonald Laboratory, Department of Physics, Kansas State University, Manhattan, KS 66506, USA

E-mail: eric.wells@augie.edu

Received 1 April 2009

Published 21 April 2009

Online at stacks.iop.org/JPhysB/42/091002

Abstract

Bond rearrangement, specifically the formation of H_2^+ and H_3^+ after ionization of methane and ammonia by fast (4 MeV) protons, is studied in both the common and deuterated isotopes of those molecules. Our coincidence time-of-flight measurements show that the relative probability of H_2^+ and H_3^+ production from ammonia is higher for the lighter isotope, contradicting the common intuition that the rearrangement occurs on the timescale of the dissociation. The isotopic effects in methane were much smaller. The relative probability of bond rearrangement leading to H_2^+ increases with the number of hydrogen atoms in the target. Unexpectedly, however, formation of H_3^+ is less likely from a methane target than from ammonia. We examined this result by calculating the ionic potential energy surface in reduced coordinates, corresponding to a symmetric stretch of a H_3^+ triangle away from the remaining C–H complex or nitrogen atom. From both the experiment and the model calculation, we find evidence to support the hypothesis that the bond rearrangement in these collisions proceeds as a two-step process in which a sudden ionization is followed by a slow molecular dissociation.

(Some figures in this article are in colour only in the electronic version)

Selective fragmentation of molecular bonds has long been a goal [1–4] of chemical control. With the use of ultrafast lasers in conjunction with pulse shapers [5, 6] and closed-loop feedback algorithms [7–9], selective ionization and fragmentation have been achieved on a number of occasions, e.g. [10–14]. The next step, forming new molecular bonds, has proven more difficult, and reports of success have been rare [15]. Further developments in this area may depend on a better understanding of the bond rearrangement process. A difficulty in stimulating selective cleavage and bond rearrangement is that the ionizing radiation that fragments the molecule often creates an unstable transient excited state of the molecular ion. Many of these excited potential energy surfaces can be

quite repulsive. Franck–Condon transitions to these surfaces therefore result in large kinetic energy release (KER) and, thus, high velocity fragments. In the case of intense-laser fragmentation, these potential energy surfaces are buffeted by the complicated time-dependent electric field of the laser as well, making it seem unlikely that a bond-rearrangement process could occur. In light of this reasoning, it is somewhat remarkable that bond rearrangement has been observed in a few cases, such as the formation of CH_3CO from $(CH_3)_2CO$ [15], the formation of H_2^+ from water [16], the formation of H_3^+ from various larger hydrocarbon molecules [17], and the isomerization of acetylene into a vinylidene dication leading to $CH_2^+ + C^+$ [18, 19].

As Mathur and Rajgara have recently pointed out [20], the technique of creating the ionizing electric field with charged particles rather than an intense laser pulse offers an alternative

³ Current address: University of South Dakota.

⁴ Current address: University of Wisconsin.

⁵ Current address: University of California, Berkeley.

method of studying bond rearrangement. For 4 MeV proton impact, the duration of the electric field seen by the few-angstrom target molecule is about 10 attoseconds, a timescale that is fast compared to any internal motions of the molecule. Thus, the extremely fast, broadband, incoherent electric field produced by fast ion impact makes an excellent baseline test for probing the mechanisms underlying bond rearrangement.

Of the rearrangement processes listed above, those leading to the formation of H_3^+ are among the most interesting. As the simplest polyatomic molecular ion, H_3^+ is a natural theoretical benchmark, but it has also attracted attention because of its central role in interstellar chemistry [21]. H_3^+ may be thought of as a hydrogen molecular ion combined with an additional hydrogen atom, forming an equilateral triangle at equilibrium with bond lengths of 1.650 [22, 23]. (Atomic units are used throughout unless otherwise specified). From the bond rearrangement perspective, the formation of H_3^+ is more complicated than the formation of H_2^+ [24–27] or the isomerization of a single proton [28–30] since more atoms and bonds are involved. Moreover, H_3^+ has an unusually complex structure for a triatomic molecule since unlike linear or bent configurations, each atom is bonded to every other atom. Despite this relative complexity, H_3^+ is known to exist in plasma environments [31] and has been observed as a product resulting from ion–molecule collisions. These collisions have involved a range of molecular targets, including very large α - and β -alanine molecules [32], methanol [33] and even methane [34, 35], which has near the minimum number of hydrogen atoms needed to form H_3^+ . Given that H_3^+ formation seems to be so general, one can reasonably ask a few questions: will H_3^+ form in a collision process in which the target has only three hydrogen atoms? Since H_3^+ is an equilateral triangle in its ground-state configuration, does it help if the parent molecule also contains a H_3^+ triangle configuration? Does the number or size of the triangles in the target change the probability of rearrangement?

Substitution of deuterated targets prompts two additional questions. First, does the timescale of the dissociation influence the probability of the rearrangement? For the same KER, deuterium atoms and ions have a lower dissociation velocity. The higher mass also restricts the size of the initial nuclear wavefunction, and therefore the vertical ionization could initially populate a different region of the ionic potential energy surface (PES). This idea underlies the explanation of isotopic effects in H_2^+ formation from water [24, 27]. Will the mechanisms leading to formation of the H_3^+ behave in a similar way?

Targets with three or more hydrogen atoms which can rearrange to form H_3^+ can also undergo a simpler process that produces H_2^+ . This offers an opportunity to compare the two processes and see if the results for the H_2^+ and H_3^+ ions follow the same trends. Our goal in this work is to build upon our experience with bond rearrangement in water [24, 25, 36–38] by examining these questions as the number of hydrogen atoms in the target molecule increases.

We have examined production of H_3^+ and H_2^+ following ionization of ammonia or methane by 4 MeV protons. Ammonia and methane have similar molecular structure, with

the fourth hydrogen atom in methane occupying the location taken by the lone electron pair attached to the nitrogen atom in ammonia. This extra proton, however, significantly increases the number of geometric combinations that could lead to bond rearrangement. Namely, in methane there are six possible ways to form H_2^+ from adjacent hydrogen pairs and four ways to form H_3^+ triangles, compared to three ways to form H_2^+ pairs and one way to form an H_3^+ triangle in the ammonia molecule. Therefore, one would intuitively expect that methane would produce more bond rearrangement than either water [24] or ammonia. Furthermore, if the rearrangement follows a slower dissociation–recombination pathway, one would assume that the proximity of the protons would play a key role, as would the dissociation velocity. In order to examine these factors, we substituted deuterated ammonia and methane in the experiment, since for the same KER, the heavier D^+ ions move more slowly. In contrast, a bond rearrangement model that emphasizes the pre-dissociation stimulation of excited bending modes in the molecule [27] might well favour the lighter isotopes because of the larger extent of the nuclear wavefunction for the less massive protons. As mentioned previously, in this model the more massive deuterium atoms have a narrower spatial distribution for their initial nuclear wave packets, making it less likely that the ionization will land them on a repulsive ionic potential energy surface (PES) that leads to bond rearrangement. Collectively, the water, ammonia and methane targets (and their isotopes) should provide an interesting set of comparative data.

Our measurement used a coincidence time-of-flight technique and apparatus that have been described in several other reports [34, 35, 39, 40] and are therefore only summarized here. A bunched beam (<2 ns bunch width) of 4 MeV protons was accelerated by the J R Macdonald Laboratory tandem Van de Graaff accelerator, collimated, and directed into a cell containing a thin target of ammonia or methane. At these velocities, electron transfer to the projectile may be neglected. It is important to note that the use of the bunched beam eliminates the need for projectile detection as part of the time-of-flight measurement, and therefore we can collect data at much higher rates, allowing analysis of less likely channels in a reasonable amount of time. The target ions produced were accelerated using a strong extraction field towards a 40 mm diameter MCP detector. The time-of-flight (TOF) spectrometer used was a two-stage Wiley–McLaren design [39, 41]. The time-of-flight of the different ions relative to a signal synchronized with the beam bunch was recorded by three time-to-amplitude converters of a multi-stop system [40]. The strong extraction field ensured that nearly all ions were collected, although this meant that the time difference between multiple fragment protons was small. As a result, we could not discern channels that included proton–proton ion pairs (or triples). For the present experiment, which was concerned mostly with H_2^+ and H_3^+ production, this problem presented little difficulty.

In the analysis of the data, we had to take into account ‘lost fragments’ due to a detector efficiency of less than 1, ^{15}N and ^{13}C isotopic abundances in our target, background contributions from residual water and air, and the rare

Table 1. Top: relative yield of the major bond rearrangement channels in 4 MeV proton collisions with ammonia targets. Relative yields are with respect to NH_3^+ (or ND_3^+), the main single ionization channel. Bottom: the same results, except for 4 MeV protons colliding with methane. Relative yields are with respect to CH_4^+ and CD_4^+ . The CH_4 results have been previously published in a different form. (Our present CH_4 results were compared to earlier data obtained with the same apparatus [34] and found to be consistent, although the earlier experiment had somewhat higher statistics. The higher statistics values are used here. The older experiment, however, did not examine any isotopic differences, and thus the results from the CD_4 target shown in table 1 are from the present experiment.)

| NH_3 | Relative yield | ND_3 | Relative yield |
|--------------------------------|----------------------------------|--------------------------------|----------------------------------|
| H_2^+ | $(3.93 \pm 0.52) \times 10^{-3}$ | D_2^+ | $(4.18 \pm 0.60) \times 10^{-3}$ |
| $\text{H}_2^+ + \text{NH}^+$ | $(2.85 \pm 0.38) \times 10^{-4}$ | $\text{D}_2^+ + \text{ND}^+$ | $(1.91 \pm 0.32) \times 10^{-4}$ |
| $\text{H}_2^+ + \text{N}^+$ | $(4.86 \pm 0.78) \times 10^{-5}$ | $\text{D}_2^+ + \text{N}^+$ | $(9.02 \pm 1.95) \times 10^{-6}$ |
| H_3^+ | $(1.13 \pm 0.12) \times 10^{-4}$ | D_3^+ | $(3.73 \pm 0.53) \times 10^{-5}$ |
| CH_4 | Relative yield | CD_4 | Relative yield |
| H_2^+ | $(4.40 \pm 0.38) \times 10^{-3}$ | D_2^+ | $(6.78 \pm 0.27) \times 10^{-3}$ |
| $\text{H}_2^+ + \text{CH}_2^+$ | $(2.3 \pm 0.3) \times 10^{-3}$ | $\text{D}_2^+ + \text{CD}_2^+$ | $(3.24 \pm 0.29) \times 10^{-3}$ |
| $\text{H}_2^+ + \text{CH}^+$ | $(1.8 \pm 0.2) \times 10^{-4}$ | $\text{D}_2^+ + \text{CD}^+$ | $(1.71 \pm 0.19) \times 10^{-4}$ |
| $\text{H}_2^+ + \text{C}^+$ | $(1.1 \pm 0.2) \times 10^{-4}$ | $\text{D}_2^+ + \text{C}^+$ | $(8.74 \pm 1.41) \times 10^{-5}$ |
| $\text{H}_3^+ + \text{CH}^+$ | $(2.0 \pm 0.3) \times 10^{-5}$ | $\text{D}_3^+ + \text{CD}^+$ | $(2.76 \pm 0.64) \times 10^{-5}$ |
| H_3^+ | $(4.80 \pm 0.50) \times 10^{-5}$ | D_3^+ | – |

occasions when one beam bunch ionized multiple target molecules. The main aspects of the necessary analysis are described in [34] and some details specific to the NH_3 and CH_4 targets are presented in our recent report of 19 MeV F^{7+} collisions with these targets [42]. Therefore, we mention only a few key details below. Compared to the highly-charged ion impact data [42], conversion to relative cross sections and fragmentation branching ratios for the present proton impact experiment were relatively straightforward because the weaker interaction reduces the amount of multiple ionization.

One analysis point to highlight is the subtraction of contributions from residual water when using CD_4 or ND_3 as a target. In these cases, there are multiple contributions to the TOF data at a mass-to-charge ratio of 18, and so the usual procedure of normalizing the H_2O^+ peaks in the target and background runs and then subtracting the residual water contribution from the target run does not work. We used two different methods of normalization in this case: (1) using the O^{2+} peak as a normalization when the O^{2+} yield was sufficient and (2) assuming the ratio of $\text{NH}_2^+/\text{NH}_3^+$ ($\text{CH}_3^+/\text{CH}_4^+$) was the same as the ratio of $\text{ND}_2^+/\text{ND}_3^+$ ($\text{CD}_3^+/\text{CD}_4^+$). Both methods yielded consistent results. The other complication, which was only a factor for the ND_3 data, was the problem of proton/deuteron exchange between the ND_3 and surfaces in the chamber, leading to the creation of ND_2H and a very small amount of NDH_2 . It is important to note that for the D_3^+ and $\text{D}_2^+ + \text{ND}^+$ channels the parent ion is unambiguous. The $\text{ND}_2\text{H}^+/\text{ND}_3^+$ ratio was evaluated to be $9.0 \pm 0.91\%$, and the correction method is described in [42]. Our main results, the relative yield of the major bond rearrangement channels resulting from 4 MeV proton collisions with ammonia and methane, are presented in table 1.

Single ionization dominates for these projectiles, so it is unsurprising that the largest channel resulting in a H_2^+ or H_3^+ from ammonia is simply H_2^+ with some combination of neutral fragments. Formation of the more complicated H_3^+ is less probable, as illustrated by the fact that the main ion-pair channel, $\text{H}_2^+ + \text{NH}^+$, is over twice as likely as single ionization

leading to H_3^+ . The $\text{H}_2^+ + \text{N}^+$ channel is nearly six times less likely than the $\text{H}_2^+ + \text{NH}^+$ channel. This decrease in probability for channels in which an extra hydrogen is liberated most likely indicates that these channels proceed through excited states which require more energy to access. This hydrogen ‘boil-off’ effect is a common theme in our data. The isotopic effects, where present, all favour more bond rearrangement in the lighter NH_3 molecule. This is similar to the behaviour reported in water [26, 37], in which H_2O exhibited the most H_2^+ production, followed by HD^+ from HDO and D_2^+ from D_2O , respectively. The channels with the largest isotopic effects are the H_3^+ and $\text{H}_2^+ + \text{N}^+$ channels. The magnitude of these isotopic effects is interesting: the measured $\text{H}_3^+/\text{D}_3^+$ ratio is 3.0 ± 0.5 , and the measured $[\text{H}_2^+ + \text{N}^+]/[\text{D}_2^+ + \text{N}^+]$ ratio is even larger, 5.4 ± 1.5 . The latter ratio indicates that the ‘boil-off’ effect mentioned above is more significant for the heavier isotopologue of ammonia, with the $\text{D}_2^+ + \text{ND}^+$ channel approximately 21 times more likely to occur than the $\text{D}_2^+ + \text{N}^+$ channel. The origin of this isotopic dependence is not completely clear, but we can suggest two avenues for investigation. First, the larger mass of the deuterium isotope decreases the amplitude of the vibrational motion compared to a hydrogen atom, thereby reducing the spatial extent of the nuclear wave packet. This reduced size could lead the wave packet to reflect off different parts of the repulsive ionic PES and hence propagate towards a different dissociation limit. Second, the wave packet propagation slows as the mass increases, and thus dynamic effects during the propagation towards the dissociation limit could play a role.

As with the ammonia target, the main bond rearrangement channels resulting from methane are the H_2^+ and $\text{H}_2^+ + \text{CH}_2^+$ channels. The branching ratio for the main ion pair channel, $\text{H}_2^+ + \text{CH}_2^+$, is surprisingly large, as has been noted previously [20, 34, 43, 44]. While the $\text{H}_2^+ + \text{NH}^+$ channel is the largest ion pair channel in ammonia, the $\text{H}_2^+ + \text{CH}_2^+$ channel in methane is about an order of magnitude more likely to occur. Comparison of the smaller bond rearrangement channels in the two targets reveals few trends. $\text{H}_2^+ + \text{N}^+$ is less likely than $\text{H}_2^+ + \text{C}^+$,

while $\text{H}_2^+ + \text{NH}^+$ is more likely than $\text{H}_2^+ + \text{CH}^+$, although one could argue that the two-body fragmentation of ammonia into $\text{H}_2^+ + \text{NH}^+$ is more properly compared to the larger $\text{H}_2^+ + \text{CH}_2^+$ channel in methane. Fragmentation of the parent molecule into additional pieces consistently reduces the probability of that final state, indicating that the ‘boil-off’ effect is present in methane as well as ammonia.

Another curious feature of the methane data is that unlike the ammonia and water cases, substitution of the more massive CD_4 increases the probability of bond rearrangement in the main channels for methane. This is, of course, what would be expected if the rearrangement occurred during the slow dissociation. The smaller bond rearrangement channels $\text{H}_2^+ + \text{CH}^+$, $\text{H}_2^+ + \text{C}^+$ and $\text{H}_3^+ + \text{CH}^+$ showed no isotopic dependence within our experimental uncertainty. The D_3^+ channel could not be isolated from the C^{2+} channel, so no isotopic comparison could be drawn.

Even more surprising is the decrease in H_3^+ production in methane compared to ammonia. Previous results from water [25], and our current results listed in table 1, show that H_2^+ production follows the trend predicted by the molecular configuration, specifically the increased number of neighbouring H–H pairs, with bond rearrangement most likely in methane and least likely in water. The measured ratio of $\text{H}_2^+/\text{H}_2\text{O}^+$ for 4 MeV proton impact is $(1.25 \pm 0.15) \times 10^{-3}$ [25]. Examination of the results presented in table 1, however, indicate that H_3^+ does not follow this intuitive trend. H_3^+ production is more likely from ammonia than methane, by a factor of 2.35 ± 0.35 . Even if the $\text{H}_3^+ + \text{CH}^+$ yield is added to the single ion H_3^+ yield in methane, H_3^+ production from ammonia is still ≈ 1.7 times more likely.

When viewed together, these results do not consistently support most common intuition about the bond rearrangement process. A slow process with the bond rearrangement proceeding dynamically during the dissociation would more readily occur with heavier isotopes and methane rather than ammonia. Both the slower moving deuterium atoms and the molecular structure of methane allow for more interaction between hydrogen nuclei during the dissociation. While some of the methane rearrangement channels support this view, the isotopic effects in ammonia and water [25] show the opposite dependence. Furthermore, adding hydrogen atoms to the system does not always increase the amount of bond rearrangement. Neither mass nor molecular configuration seems to provide a simple argument that can predict the amount of bond rearrangement that might occur.

We suggest that this dilemma can be resolved by viewing the bond rearrangement process as an initial sudden ionization mechanism followed by dissociation. In this model, rapid ionization causes a vertical transition to the ionic PES of the molecule upon which the nuclear wave packet may propagate. Essentially, the probability of bond rearrangement involving the hydrogen atoms in ammonia or methane depends on the molecular configuration at the instant of the sudden ionization step.

We tested this model to see if it could explain the relative amounts of H_3^+ production in methane and ammonia. In order to carry out this analysis we examined the PES for

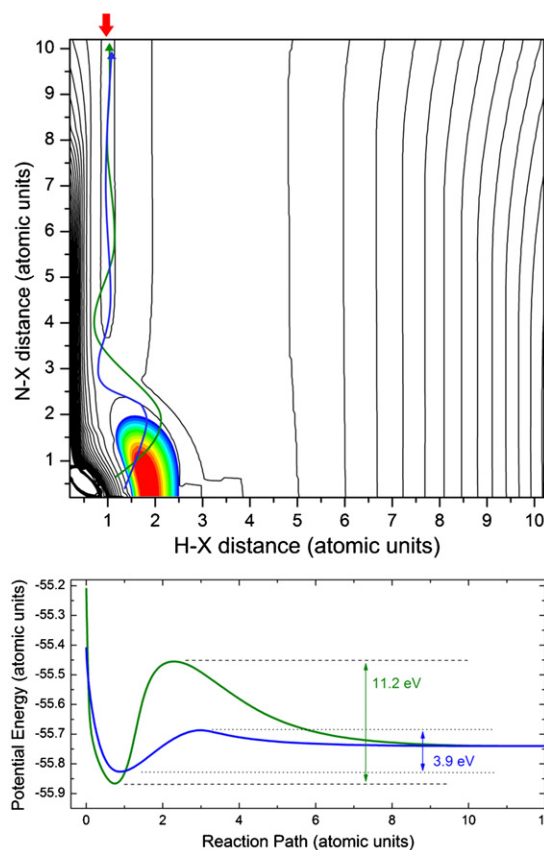


Figure 1. Top: the NH_3^+ potential energy surface in reduced coordinates. The contour intervals are 0.166 atomic units. ‘X’ refers to the centre of mass of the H_3^+ triangle. The equilibrium bond length for an H_3^+ ion corresponds to an H–X value of 0.95, designated by the red arrow above the plot. The colour plot represents the equilibrium vibrational population of NH_3 superimposed on the ionic potential energy surface. The green line illustrates a typical trajectory (or reaction path) for wave packet propagation off the repulsive part of the NH_3^+ PES leading to the N + H_3^+ dissociation limit. The blue line shows an alternative path off the repulsive surface originating at a small N–X distance. Bottom: the energy of the ionic PES as a function of the reaction path for the two arrows drawn in the top figure. While both paths emerge near the equilibrium size of ground state H_3^+ , the blue arrow faces a smaller activation barrier.

ammonia and methane, explicitly examining a symmetric stretch configuration of the H_3^+ triangle away from the nitrogen atom or C–H complex. Using the Gaussian03 commercial software package [45], we carried out *ab initio* all electron calculations for the lowest energy structures of NH_3 , NH_3^+ , CH_4 and CH_4^+ , using fifth-order Möller–Plesset perturbative calculations and a correlation-consistent polarized valence double-zeta basis set [46]. To test the PES calculation, we carried out a geometry optimization for the NH_3 and CH_4 PES and found the minimum energy configurations for C_{3v} and T_d symmetries, respectively, as expected. The results of our PES calculation for NH_3 are shown in figure 1. The contours show the NH_3^+ PES, and the colours represent the ground-state nuclear wavefunction superimposed onto the PES. Figure 1 is a cut through the NH_3^+ PES for a symmetric stretch. The coordinates are with respect to the centre of mass of the H_3^+ triangle, which we designate as X. The ground state separation

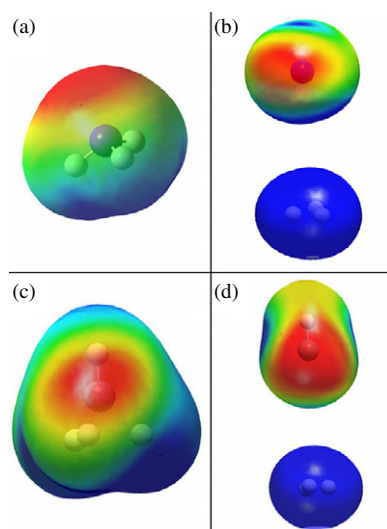


Figure 2. Top: calculated electron densities for NH_3^+ at two locations on the cut through the PES shown in figure 1: (a) at the NH_3^+ equilibrium location and (b) at $\text{H-X} = 1.0$ and $\text{N-X} = 9.4$, at which point the N and H_3^+ are separated. Red is high electron density, blue is low electron density. Bottom: the same calculations for methane, with (c) near equilibrium and (d) at $\text{H-X} = 1.0$ and $\text{C-X} = 10.05$.

of the protons in H_3^+ of 1.65 corresponds to a H-X distance of 0.95. In this representation, the N-X coordinate is the distance of the nitrogen atom from the centre of the H_3^+ triangle, and the H-X coordinate represents the size of the H_3^+ triangle. The dissociation pathway leading to H_3^+ production along this surface would then end at a large N-X value and at an H-X value near equilibrium for H_3^+ , i.e. around $\text{H-X} = 0.95$, as designated by the red arrow above the contour plot in figure 1. To verify that this path would lead to $\text{N} + \text{H}_3^+$ and not $\text{N}^+ + 3\text{H}$, we calculated the electron density of the NH_3^+ ion near equilibrium ($\text{H-X} = 1.0$) and at a large N-X value. As shown in figure 2, the configuration at that location is indeed $\text{N} + \text{H}_3^+$.

We have carried out similar calculations for methane, with the results shown in figures 2 and 3. In the cut through the CH_4^+ PES, shown in figure 3, we chose one hydrogen to stay with the carbon atom, while the other three hydrogen atoms symmetrically move away from the carbon, leading to a $\text{H}_3^+ + \text{CH}$ final state. Both PES calculations show that the centre of the neutral molecule's nuclear wavefunction is approximately centred on the minimum of the ionic PES. As a result, the pathways leading to the bond rearrangement outcome are uphill, and thus only ions that are initially in highly excited vibrational states can dissociate along these pathways, because only this non-equilibrium population overlaps the repulsive part of the ionic PES. As a result, these fragments should have a relatively low KER, a conclusion that is supported by our data [42].

Two points from these PES calculations support the observation that H_3^+ production from ammonia is more likely than from methane. First, the equilibrium bond length in H_3^+ of 1.65 (which corresponds to $\text{H-X} = 0.95$) lies close to a local minimum on the NH_3^+ PES. Thus, if part of the population makes it out of the equilibrium well on that surface heading towards large N-X , it is energetically favourable for

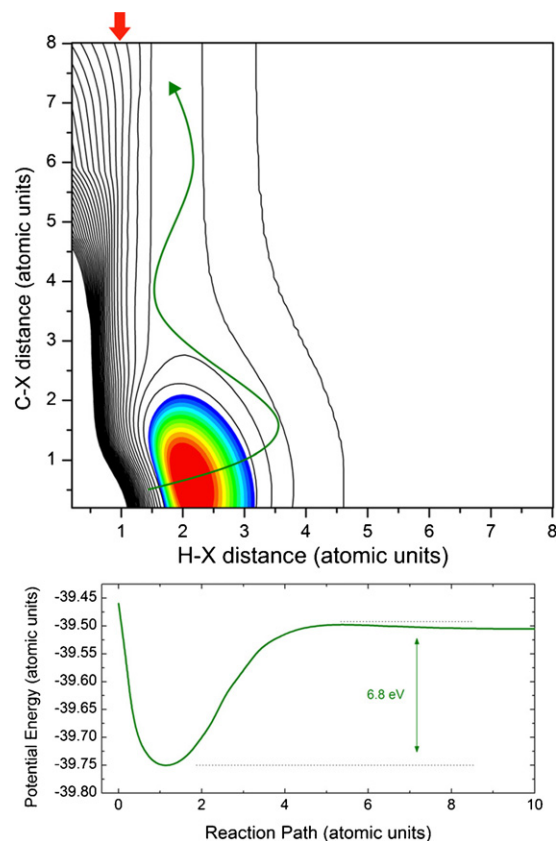


Figure 3. Similar to figure 1, but for methane. Top: the CH_4^+ potential energy surface in reduced coordinates. The contour intervals are 0.055 atomic units. 'X' refers to the centre of mass of the H_3^+ triangle. The red arrow marks the equilibrium bond length for the H_3^+ ion which corresponds to $\text{H-X} = 0.95$. We have treated one hydrogen atom as fixed to the carbon atom, as shown in figure 2 and allowed the remaining H_3^+ triangle to stretch symmetrically. The green arrow shows a typical path for the wave packet propagation that could lead to formation of H_3^+ . Bottom: energy versus reaction path distance for the green arrow in the top plot.

the population to proceed towards a geometry consistent with stable H_3^+ formation. On the CH_4^+ surface, the $\text{H-X} = 0.95$ point is located further up the repulsive hill, and population would tend to be kicked out towards larger H-X values. This would correspond to H_3^+ in excited vibrational states, which may tend to fall apart. Certainly, larger H-X distances seem to be more accessible on our calculated CH_4^+ PES than the NH_3^+ PES, because the CH_4^+ PES becomes nearly flat for H-X values above ≈ 5 . Second, the energy difference between the equilibrium of the CH_4^+ PES and the $\text{CH} + \text{H}_3^+$ final state is around 6.5 eV, with the barrier being around 6.8 eV, as shown in figure 3. Most potential wave packet paths along this surface to the $\text{CH} + \text{H}_3^+$ dissociation limit have roughly the same energetic considerations. For NH_3^+ , however, the difference between equilibrium and the $\text{N} + \text{H}_3^+$ dissociation limit is only 4.35 eV, although for most possible wave packet paths, the barrier is much higher, over 11 eV. The repulsive surface curves slightly at very small N-X distances, however, leading to the possibility of a more energetically favourable path, with a barrier of less than 4 eV. This is illustrated in figure 1. Coupled together, these two

observations form a plausible explanation for the relative differences in H_3^+ production between the two targets.

There are, of course, some issues that our model calculations do not address. First, there are other possible dissociation pathways leading to the production of H_3^+ , such as asymmetric stretching modes, that we have not considered. In addition, analysis of the population evolution on the ionic PES was crude, merely pointing out various possible paths and considering the energy barriers involved. We made no attempt to perform a proper wave packet propagation calculation along the PES and determine the relative probabilities for different possible final states. We hope that this initial work will motivate a more rigorous theoretical treatment.

These data, combined with the recent work on water [25], suggest that a two-step picture of bond rearrangement, in which a sudden ionization is followed by a relatively slow dissociation, may often be applicable to small polyatomic molecules exposed to swift electric fields. In this picture, the sudden ionization step influences the second dissociative step because the location of the nuclear wave packet at the time of the rapid ionization event defines the population distribution on the ionic PES and thus initial conditions for the wave packet propagation along the ionic PES. If this analysis is true, two interesting points can be made with respect to future experiments. First, advances in attosecond technology [47] make it possible to consider pump–probe experiments [48] that can initiate and then track the time evolution of the wave packet along the ionic PES of small polyatomic molecules. Second, from the point of view of controlling the rearrangement process, shifting the nuclear wavefunction to a more advantageous non-equilibrium position prior to the ionization step could prove more profitable than trying to manipulate the wave packet on the ionic PES during the post-ionization part of the process. Some of the isotopic effects in ammonia and methane, however, suggest that the details of the ionic PES and the wave packet propagation can influence the probability of bond rearrangement as well. Therefore, a two-step picture of bond rearrangement (i.e., a rapid ionization followed by a slow dissociation) in which either step may determine the amount of rearrangement, gives the most comprehensive picture of the bond rearrangement process.

In summary, we have examined the bond rearrangement channels leading to the production of H_2^+ and H_3^+ ions from methane and ammonia following collisions with 4 MeV protons. In order to examine the dependence on the dissociation velocity, we substituted CD_4 and ND_3 for CH_4 and NH_3 . We find that ionizing collisions with NH_3 are more likely to produce H_2^+ and H_3^+ than collisions with ND_3 . While these results are similar to recent results for water molecules [25], they are counterintuitive if one imagines that the rearrangement occurs on the timescale of the dissociation. In contrast, the isotopic effects observed in methane ($D_2^+ > H_2^+$ and $CD_2^+ + D_2^+ > CH_2^+ + H_2^+$) favour bond rearrangement from CD_4 . Final states in which bond rearrangement occurs and one or more additional protons are liberated are less likely than final states that only involve a bond rearrangement. This ‘boil-off’ effect is evident in both isotopologues of methane and ammonia.

Our results also fail to follow an intuitive assessment based on increasing the number of hydrogen triangles, with more H_3^+ produced in ammonia than methane. Our model calculations suggest that the sudden ionization step is responsible for this surprising observation. These results, coupled with similar work on H_2O [25], indicate that either the details of the nuclear wave packet at the time of the sudden ionization or the specifics of the wave packet propagation on the ionic potential energy surface can influence the amount of bond rearrangement. Thus, when considering the bond rearrangement process in a molecule, neither of these steps should be dismissed *a priori*.

Acknowledgments

We thank Nora G Johnson, Nate Jastram and Ivan Lee for their assistance with data collection and Brett Esry for useful discussions. This work was supported by Research Corporation, National Science Foundation award PHY-0653598 and the Chemical Sciences, Geosciences, and Biosciences Division, Office of Basic Energy Science, US Department of Energy. SC and EW acknowledge additional support provided by the National Science Foundation—Undergraduate Research Center program: CHE-0532242 ‘The Northern Plains Undergraduate Research Collaboration (NPURC)’.

References

- [1] DeWitt M J and Levis R J 1995 *J. Chem. Phys.* **102** 8670
- [2] DeWitt M J, Peters D W and Levis R J 1997 *Chem. Phys.* **218** 211
- [3] Ledingham K W D *et al* 1998 *J. Phys. Chem. A* **102** 3002
- [4] Smith D J *et al* 1998 *Rapid Commun. Mass Spectrom.* **12** 813
- [5] Weiner A M, Leaird D E, Patel J S and Wullert J R 1990 *Opt. Lett.* **15** 326
- [6] Wefers M M and Nelson K A 1993 *Opt. Lett.* **18** 2032
- [7] Judson R S and Rabitz H 1992 *Phys. Rev. Lett.* **68** 1500
- [8] Pearson B J, White J L, Weinacht T C and Bucksbaum P H 2001 *Phys. Rev. A* **63** 063412
- [9] Zeidler D, Frey S, Kompa K-L and Motzkus M 2001 *Phys. Rev. A* **64** 023420
- [10] Assion A *et al* 1998 *Science* **282** 919
- [11] Bergt M, Brixner T, Kiefer B, Strehle M and Gerber G 1999 *J. Phys. Chem. A* **103** 10381
- [12] Wells E *et al* 2005 *Phys. Rev. A* **72** 063406
- [13] Cardoza D, Baertschy M and Weinacht T 2005 *J. Chem. Phys.* **123** 074315
- [14] Cardoza D, Pearson B J, Baertschy M and Weinacht T C 2006 *J. Photochem. Photobiol. A: Chem.* **180** 277
- [15] Levis R J, Menkir G M and Rabitz H 2001 *Science* **292** 709
- [16] Rottke H, Trump C and Sandner W 1998 *J. Phys. B: At. Mol. Opt. Phys.* **31** 1083
- [17] Hoshina K, Furukawa Y, Okino T and Yamanouchi K 2008 *J. Chem. Phys.* **129** 104302
- [18] Alnaser A S *et al* 2006 *J. Phys. B: At. Mol. Opt. Phys.* **39** S485
- [19] Hishikawa A, Matsuda A, Fushitani M and Takahashi E J 2008 *Phys. Rev. Lett.* **99** 258302
- [20] Mathur D and Rajgara F A 2006 *J. Chem. Phys.* **124** 194308
- [21] Watson J K G 2000 *Phil. Trans. R. Soc. Lond. A* **358** 2371
- [22] Cencek W, Rychlewski J, Jaquet R and Kutzelnigg W 1998 *J. Chem. Phys.* **108** 2831

- [23] Jaquet R, Cencek W, Kutzelnigg W and Rychlewski J 1998 *J. Chem. Phys.* **108** 2837
- [24] Ben-Itzhak I *et al* 2005 *Nucl. Instrum. Methods Phys. Res. B* **233** 284
- [25] Ben-Itzhak I *et al* 2009 *Phys. Rev. A*, to be submitted
- [26] Straub H C, Lindsay B G, Smith K A and Stebbings R F 1998 *J. Chem. Phys.* **108** 109
- [27] Piancastelli M N *et al* 1999 *Phys. Rev. A* **59** 300
- [28] Osipov T *et al* 2003 *Phys. Rev. Lett.* **90** 233002
- [29] Flammini R, Fainelli E, Maracci F and Avaldi L 2008 *Phys. Rev. A* **77** 044701
- [30] Zyubina T S, Dyakov Y A, Lin S H, Bandrauk A D and Mebel A M 2005 *J. Chem. Phys.* **123** 134320
- [31] McCall B J and Oka T 2000 *Science* **287** 1941
- [32] Bari S *et al* 2008 *J. Chem. Phys.* **128** 074306
- [33] De S, Rajput J, Roy A, Ghosh P N and Safvan C P 2006 *Phys. Rev. Lett.* **97** 213201
- [34] Ben-Itzhak I *et al* 1993 *Phys. Rev. A* **47** 3748
- [35] Ben-Itzhak I, Carnes K D, Johnson D T, Norris P J and Weaver O L 1994 *Phys. Rev. A* **49** 881
- [36] Sayler A M, Wells E, Carnes K D and Ben-Itzhak I 2001 *Application of Accelerators in Research and Industry (AIP Conf. Proc. vol 576)* ed J L Duggan and I L Morgan (New York: American Institute of Physics) pp 33–5
- [37] Sayler A M, Maseberg J W, Hathiramani D, Carnes K D and Ben-Itzhak I 2003 *Application of Accelerators in Research and Industry (AIP Conf. Proc. vol 576)* ed J L Duggan and I L Morgan (New York: American Institute of Physics) pp 48–51
- [38] Sayler A M *et al* 2006 *J. Phys. B: At. Mol. Opt. Phys.* **39** 1701
- [39] Ben-Itzhak I, Ginther S G and Carnes K D 1992 *Nucl. Instrum. Methods Phys. Res. B* **66** 401
- [40] Ben-Itzhak I, Carnes K D and DePaola B D 1992 *Rev. Sci. Instrum.* **63** 5780
- [41] Wiley W C and McLaren I H 1955 *Rev. Sci. Instrum.* **26** 2903
- [42] Wells E *et al* 2009 *Application of Accelerators in Research and Industry (AIP Conf. Proc. vol 1099)* ed F Del McDaniel and B M Doyle (New York: American Institute of Physics) pp 133–6
- [43] McCulloh K E, Sharp T E and Rosenstock H M 1965 *J. Chem. Phys.* **42** 3501
- [44] Backx C and Van der Weil M J 1975 *J. Phys. B: At. Mol. Phys.* **8** 3020
- [45] Frisch M J *et al* 2003 GAUSSIAN 2003, Gaussian, Inc., Wallingford, CT, 2003
- [46] Woon D E and Dunning T H 1993 *J. Chem. Phys.* **98** 1358
- [47] Goulielmakis E *et al* 2008 *Science* **320** 1614
- [48] Alnaser A S *et al* 2005 *Phys. Rev. A* **72** 030702